

Log-Poisson Hierarchical Clustering of Cosmic Neutral Hydrogen and Ly α Transmitted Flux of QSO Absorption Spectrum

Yi Lu^{1,2}, Yao-Quan Chu¹, and Li-Zhi Fang²

ABSTRACT

We study, in this paper, the non-Gaussian features of the mass density field of neutral hydrogen fluid and the Ly α transmitted flux of QSO absorption spectrum from the point-of-view of self-similar log-Poisson hierarchy. It has been shown recently that, in the scale range from the onset of nonlinear evolution to dissipation, the velocity and mass density fields of cosmic baryon fluid are extremely well described by the She-Leveque's scaling formula, which is due to the log-Poisson hierarchical cascade. Since the mass density ratio between ionized hydrogen to total hydrogen is not uniform in space, the mass density field of neutral hydrogen component is not given by a similar mapping of total baryon fluid. Nevertheless, we show, with hydrodynamic simulation samples of the concordance Λ CDM universe, that the mass density field of neutral hydrogen, is also well described by the log-Poisson hierarchy.

We then investigate the field of Ly α transmitted flux of QSO absorption spectrum. Due to redshift distortion, Ly α transmitted flux fluctuations are no longer to show all features of the log-Poisson hierarchy. However, some non-Gaussian features predicted by the log-Poisson hierarchy are not affected by the redshift distortion. We test these predictions with the high resolution and high S/N data of quasars Ly α absorption spectra. All results given by real data, including β -hierarchy, high order moments and scale-scale correlation, are found to be well consistent with the log-Poisson hierarchy. We compare the log-Poisson hierarchy with the popular log-normal model of the Ly α transmitted flux. The later is found to yield too strong non-Gaussianity at high orders, while the log-Poisson hierarchy is in agreement with observed data.

Subject headings: cosmology: theory - large-scale structure of universe

¹Center for Astrophysics, University of Science and Technology of China, Hefei, Anhui 230026, China

²Department of Physics, University of Arizona, Tucson, AZ 85721

1. Introduction.

Baryon matter of the universe is mainly in the form of intergalactic medium (IGM), of which the dynamics can be described as compressible fluid. Luminous objects are formed from baryon matter in the gravitational well of dark matter. Therefore, the dynamical state of baryon fluid in nonlinear regime is crucial to understand the formation and evolution of the large scale structures of the universe. In the linear regime, the baryon fluid follows the mass and velocity fields of collisionless dark matter. In the nonlinear regime, however, the baryon fluid statistically decouples from the underlying dark matter field. The statistical behavior of baryon fluid is no longer described by a similar mapping of the underlying dark matter field (e.g. Pando et al. 2004).

It was first pointed out by Shandarin and Zeldovich (1989) that the dynamical behavior of baryon matter clustering on large scales is similar to turbulence. The expansion of the universe eliminates the gravity of uniformly distributed dark matter. The motion of baryon matter on scales larger than dissipation is like that of matter moving by inertia. In this regime, the evolution of baryon matter is scale-free and dynamically like fully developed turbulence in inertial range. The turbulence of incompressible fluid leads the energy passes from large to the smallest eddies, and finally dissipates into thermal motion. While the clustering of cosmic baryon fluid is also due to the transform of density perturbations on different scales, and finally falls and dissipates into virialized halos of dark matter. Yet, the turbulence of incompressible fluid is rotational (Landau & Lifshitz 1987), while the clustering of cosmic matter is irrotational, because vorticities do not grow in an expanding universe (Peebles 1980).

Nevertheless, the turbulence-like behavior of cosmic baryon fluid has been gradually noticed. First, the dynamics of growth modes of the cosmic matter is found to be sketched by a stochastic force driven by Burger's equation (Gurbatov, et al 1989, Berera & Fang, 1994). The Burger's equation driven by the random force of the gravity of dark matter can also sketch the evolution of baryon fluid, if cooling and heating are ignored (Jones 1999; Matarrese & Mohayaee 2002). Later, the Burger's fluid is found to show turbulence behavior if the Reynolds number is large enough (Polyakov 1995; Lassig 2000; Bec & Frisch 2000; Davoudi et al. 2001). The Reynolds number of IGM at nonlinear regime actually is large. Therefore, we may expect that, in the scale free range, the dynamical state of cosmic baryon fluid should be Burger's turbulence. The turbulence of Burger's fluid is different from the turbulence of incompressible fluid. The later consists of vortices on various scales, while the former is a collection of shocks.

With the cosmological hydrodynamic simulation based on Navier-Stokes equations in which heating and cooling processes are properly accounted, it has been found that the

velocity field of the IGM consists of an ensemble of shocks, and satisfies some scaling relations predicted by Burger’s turbulence (Kim et al. 2005). This result reveals that the turbulence features of cosmic baryon fluid are independent of the details of dissipation (heating and cooling) mechanism if we consider only the scale free range, i.e. from the scale of the onset of nonlinear evolution to the scale of dissipation, say Jeans length.

A new progress is to show that the velocity field of cosmic baryon fluid can extremely well described by She-Leveque’s (SL) scaling formula (He et al. 2006). The SL formula is considered to be the basic statistical features of the self-similar evolution of fully developed turbulence. Very recently, the non-Gaussianities of mass density field of the hydrodynamic simulation samples are found to be well consistent with the predictions of the log-Poisson hierarchy, which originates from some hidden symmetry of the Navier-Stokes equations. This hierarchical model gives a unified explanation of non-Gaussian features of baryon fluid, including the intermittence, hierarchical relation, scale-scale correlations etc (Liu & Fang 2008). These results strongly indicate that, in the scale free range, dynamical state of cosmic baryon fluid is similar to a fully developed turbulence.

In this paper, we investigate the log-Poisson hierarchy of cosmic baryon fluid with observed data – the Ly α transmitted flux of quasar absorption spectrum, which is due to the absorptions of quasar continuum by the diffusely distributed neutral hydrogen (Bi et al 1995, Bi & Devidsen 1997, Rauch 1998). These samples offer a unique way to study the non-Gaussian feature of cosmic baryon fluid. It has been known for a long time that the fields of Ly α forests and transmitted flux are highly non-Gaussian. Observation samples of Ly α forests and transmitted flux show scale-scale correlation (Pando et al 1998), intermittence (Jamkhedkar et al. 2000; Pando et al. 2002; Feng et al. 2003), non-thermal broadening of H I and He II Ly α absorption lines (Zheng et al. 2004; Liu et al. 2006). We will show that the log-Poisson hierarchy provides a crux to understand the non-Gaussian behavior.

The outline of this paper is as follows. §2 gives an introduction of the log-Poisson hierarchy. §3 shows that the neutral hydrogen component of cosmic baryon fluid is of log-Poisson hierarchy. In §4, we study the log-Poisson hierarchy of the field of Ly α transmitted flux with observed samples of quasar absorption spectra. A comparison between log-Poisson hierarchy and log-normal model is also presented in §4. The conclusion and discussion are given in §5.

2. Log-Poisson hierarchy

2.1. Structure function

To describe the statistical properties of an isotropic and homogenous random field $\rho(\mathbf{x})$, it generally uses correlation functions of $\delta\rho(\mathbf{x}) = \rho(\mathbf{x}) - \bar{\rho}$, $\bar{\rho}$ being the mean of density. For instance, a two-point correlation function is $\langle \delta\rho(\mathbf{x})\delta\rho(\mathbf{x}') \rangle$. To reveal the turbulence-like behavior, we use variable $\delta\rho_r = \rho(\mathbf{x} + \mathbf{r}) - \rho(\mathbf{x})$, where $r = |\mathbf{r}|$. The variable $\delta\rho_r$ is very different from variable $\delta\rho(\mathbf{x})$. The later can be larger than $\bar{\rho}$, but cannot be less than $-\bar{\rho}$, and therefore, for a nonlinear field, the distribution of $\delta\rho(\mathbf{x})$ generally is skew; however, the distribution of $\delta\rho_r$ is symmetric with respect to positive and negative $\delta\rho_r$ if the field is statistically uniform.

With $\delta\rho(\mathbf{x})$ the clustering and non-Gaussianity of mass density $\rho(\mathbf{x})$ are measured by two and multiple point correlation functions of $\delta\rho(\mathbf{x})$. With $\delta\rho_r$, the statistical features are described by structure function defined as

$$S_p(r) \equiv \langle |\delta\rho_r|^p \rangle, \quad (1)$$

where p is the order of statistics, and the average $\langle \dots \rangle$ is taken over the ensemble of density field. A comparison of the correlation function and structure function has been analyzed in detail by Monin & Yaglom (1975). The 2nd structure function $S_2 = \langle |\delta\rho_r|^2 \rangle$ as a function r (scale) actually is the power spectrum of the mass density field $\rho(\mathbf{r})$ (Fang & Feng 2000).

In the scale-free range of the dynamical equations and initial conditions, the structure function is scale-invariant, and therefore, it is generally expressed as a power law of r

$$S_p(r) \propto r^{\xi(p)}. \quad (2)$$

$\xi(p)$ is called intermittent exponent. Since the pioneer work of Kolmogorov (1941), it is believed that the relation of $\xi(p)$ vs. p is related to the scale-covariance of the dynamical equations and initial conditions. For fully developed turbulence of Navier-Stokes fluid, $\xi(p)$ is a nonlinear function of p . Since then many hierarchy models for interpreting $\xi(p)$ have been proposed (Frisch 1995). Finally the best model is given by the SL scaling formula (She & Leveque 1994), which is yielded from the Log-Poisson hierarchy process (Dubrulle 1994).

Although the cosmic baryon fluid is not incompressible, samples of mass and velocity fields of cosmic baryon fluid produced by the cosmological hydrodynamic simulation of the concordance Λ CDM model show in good arggement with the SL scaling and log-Poisson hierarchy. This is not surprising, because the hierarchical structure model is mainly based on the invariance and symmetry of nonlinear dynamical systems. Therefore, systems other

than the Navier-Stokes incompressible fluid will also show the SZ scaling and log-Poisson hierarchy if they have the similar invariance and symmetry (She 1997).

2.2. Log-Poisson hierarchical cascade

The scenario of hierarchical clustering has been widely used to describe nonlinear evolution of the mass field of cosmic matter. We will first give the basic assumptions of log-Poisson hierarchy cascade, and then discuss the physics behind this model.

The log-Poisson hierarchy assumes that, in the scale free range, the variables (density fluctuation) $|\delta\rho_r|$ on different scales r are related by a statistical relation as (Dubrulle 1994, She & Waymire 1995),

$$|\delta\rho_{r_2}| = W_{r_1 r_2} |\delta\rho_{r_1}|, \quad (3)$$

where

$$W_{r_1 r_2} = \beta^m (r_1/r_2)^\gamma. \quad (4)$$

In eqs.(3) and (4), $r_1 \geq r_2$, and m is a random variable with the Poisson PDF as

$$P(m) = \exp(-\lambda_{r_1 r_2}) \lambda_{r_1 r_2}^m / m!. \quad (5)$$

To insure the normalization $\langle W_{r_1 r_2} \rangle = 1$, where $\langle \dots \rangle$ is over m , the mean $\lambda_{r_1 r_2}$ of the Poisson distribution should be

$$\lambda_{r_1 r_2} = \gamma [\ln(r_1/r_2)] / (1 - \beta). \quad (6)$$

The model eq.(3) describes how a density fluctuation $|\delta\rho_{r_1}|$ on larger scale r_1 statistically related to fluctuation $|\delta\rho_{r_2}|$ on smaller scale r_2 . The log-Poisson model depends only on the ratio r_1/r_2 . Thus, it is scale invariant. The random variable m can be considered as the steps of the evolution from $|\delta\rho_{r_1}|$ to $|\delta\rho_{r_2}|$. When β is smaller, only the evolutionary process with lower steps is important.

For a Gaussian field, variables $\delta\rho_{r_1}$ and $\delta\rho_{r_2}$ have to be statistically independent. It likes that the Fourier modes with different wavenumber $k_1 \propto 1/r_1$ and $k_2 \propto 1/r_2$ are statistically independent. Therefore, a Gaussian field has to be $\beta = 1$. Thus, the parameters $\beta < 1$ is a measure of the deviation from Gaussian field. The meaning of γ will be given later.

Among hierarchical clustering models, the log-Poisson hierarchy has the following features. First, the relation between $|\delta\rho_{r_1}|$ and $|\delta\rho_{r_2}|$ given by eq.(3) is a multiplicative random process. A random multiplicative cascade generally yields a non-Gaussian field. That is, even the field on large scale r_1 is Gaussian, it will be non-Gaussian on small scale r_2 . This

is different from additive random process (e.g. Cole & Kaiser 1988), which generally yields Gaussian field (Pando et al. 1998).

Second, the cascade from scale r_1 to r_2 , and then to r_3 is identical to the cascade from r_1 to r_3 . It is because $W_{r_1 r_3} = W_{r_1 r_2} W_{r_2 r_3} = \beta^N (r_1/r_3)^\gamma$, where N is again a Poisson random variable with $\lambda_{r_1 r_3} = \lambda_{r_1 r_2} + \lambda_{r_2 r_3}$. Therefore, the log-Poisson hierarchy removes an arbitrariness in defining the steps of cascade from r_1 to r_2 or r_2 to r_3 . This arbitrariness is a major shortcoming of many hierarchical clustering models, one of them, for instance, is the clustering hierarchy models (Soneira & Peebles 1977, Peebles 1980).

Third, although the log-Poisson hierarchical process is discrete in terms of the discrete random number m , it is infinitely divisible. That is, there is no lower limit on the difference $r_1 - r_2$. It can be infinitesimal. This is consistent with the continuous variable r used in the hydrodynamic equation of cosmic baryon fluid. The infinite divisibility can not be modeled with hierarchy of discrete objects with finite size. Log-normal model is also infinitely divisible. However, their asymptotic behavior of $\xi(p)$ at larger p is unbound. We will compare the log-normal model with log-Poisson in §4.4.

2.3. Intermittent exponent

With log-Poisson hierarchy eq.(3), the intermittent exponent $\xi(p)$ is found to be (Liu & Fang 2008)

$$\xi(p) = -\gamma[p - (1 - \beta^p)/(1 - \beta)]. \quad (7)$$

When $\beta \rightarrow 1$, we have $\xi(p) = 0$. Therefore, $\beta = 1$ is a Gaussian field. A field with $\beta < 1$ is called intermittent. Eq.(7) requires $\xi(1) = 0$. Therefore, the difference of an intermittent field from Gaussian is mainly given by the term $\gamma(1 - \beta^p)/(1 - \beta)$ of eq.(7).

From eq.(7), the power spectrum $S_2(r) = \text{const}$ is flat. This is not generally applicable for the cosmic density field. In the scale free range, the power spectrum of mass field is of power-law. Thus, we should generalize the log-Poisson hierarchy eq.(3) by replacing $\delta\rho_{r_1}$ and $\delta\rho_{r_2}$ with $r_1^\alpha \delta\rho_{r_1}$ and $r_2^\alpha \delta\rho_{r_2}$. In this case, the intermittent exponent $\xi(p)$ is

$$\xi(p) = -\alpha p - \gamma[p - (1 - \beta^p)/(1 - \beta)]. \quad (8)$$

Eqs.(2) and (7) yield $S_2(r) \propto r^{-2\alpha}$, and therefore, the parameter 2α is the index of power spectrum. When $\alpha = 0$, eq.(8) is the same as eq.(7).

2.4. β -hierarchy

Since $|\delta\rho_r|^p$ is the p -th moment of the $\delta\rho_r$, for high p , one can attribute the structure function $S_p(r)$ to the events located at the tail of the probability distribution function (PDF) of $\delta\rho_r$. To pick up the structures, which dominant the p -order statistics of $\delta\rho_r$, we define

$$F_p(r) \equiv S_{p+1}(r)/S_p(r). \quad (9)$$

From equations (2) and (8), equation (9) gives

$$F_p(r) = Ar^{-\alpha-\gamma(1-\beta^p)}. \quad (10)$$

where the constant A is independent of r and p . For an intermittent field $\beta < 1$, we have $F_\infty(r) = Ar^{-\alpha-\gamma}$. Thus, from eq.(10), one can find

$$\frac{F_p(r)}{F_\infty(r)} = \left[\frac{F_{p+1}(r)}{F_\infty(r)} \right]^{1/\beta}, \quad (11)$$

Equation (11) is invariant with respect to a translation in p . Since $F_p(r)$ measures the structures dominating the p order statistics, the larger the p , the larger the contribution of strong-clustered structures to $F_p(r)$. Therefore, equation (11) describes the hierarchical relation between the stronger (or high p) and weaker (or low p) clustering. In the scale-free range where $F_{p+1}(r)/F_\infty(r) < 1$, we have $F_p(r)/F_\infty(r) < F_{p+1}(r)/F_\infty(r)$ if $\beta < 1$. That is, for an intermittent field, weak clustering structures are strongly suppressed with respect to the strong clustering; the smaller the β , the stronger the suppression of weak clustering structures.

From eq.(11), we have

$$\ln F_{p+1}(r)/F_3(r) = \beta \ln F_p(r)/F_2(r). \quad (12)$$

This, for *all* r and p , $\ln[F_{p+1}(r)/F_3(r)]$ vs. $\ln[F_p(r)/F_2(r)]$ should be on a straight line with slope β . It is called β -hierarchy. Eq.(12) does not contain parameter γ and term $F_\infty(r)$, and therefore, it is a testable prediction of the log-Poisson hierarchy.

Therefore, log-Poisson hierarchy links the sizes of fluctuation structures [eq.(3)] as well as their amplitude or intensity [eq.(11)]. This is different from hierarchy models, which give only the relationship between the sizes of objects. The hierarchical relation eq.(11) actually is the origin of the log-Poisson hierarchy. That is, the hierarchical relation like eq.(11) is the first recognized to be held for dynamical system described by the Navier-Stokes equations, or equations close to the Navier-Stokes fluid (Dubrulle 1994, Leveque & She 1997). Therefore, the SL formula has also been successfully applied to describe the mass fields of compressible fluid (Boldyrev et al 2002, Padoan et al 2003).

2.5. γ -related non-Gaussianities

The ratio between higher order to second order moments $\langle \delta \rho_r^{2p} \rangle / \langle \delta \rho_r^2 \rangle^p$ is a popular tool to measure non-Gaussianity. When $p = 2$, the ratio is kurtosis. For a Gaussian field, the ratio is independent of r , and equal to

$$\frac{\langle \delta \rho_r^{2p} \rangle}{\langle \delta \rho_r^2 \rangle^p} = (2p - 1)!! \quad (13)$$

For log-Poisson hierarchy, one can show (Liu & Fang 2008)

$$\ln \frac{\langle \delta \rho_r^{2p} \rangle}{\langle \delta \rho_r^2 \rangle^p} = K_p \ln r + \text{const} \quad (14)$$

The moment ratio $\ln(\langle \delta \rho_r^{2p} \rangle / \langle \delta \rho_r^2 \rangle^p)$ is linearly dependent on $\ln r$ (scale free) with the slope K_p given by

$$K_p = -\gamma \frac{p(1 - \beta^2) - (1 - \beta^{2p})}{1 - \beta} \quad (15)$$

As expected, for Gaussian field ($\beta \rightarrow 1$), $K_p = 0$, i.e. the ratio of moments is independent of r [Eq.(14)]. That is, K_p only depends on the last term on the right hand side of eq.(8), regardless the parameter α .

Other useful non-Gaussian detector is the scale-scale correlation defined as

$$C_{r_1, r_2}^{p, p} \equiv \frac{\langle \delta \rho_{r_1}^p \delta \rho_{r_2}^p \rangle}{\langle \delta \rho_{r_1}^p \rangle \langle \delta \rho_{r_2}^p \rangle}, \quad (16)$$

which describes the correlation between the density fluctuations on scales r_1 and r_2 . Obviously, for a Gaussian field, $C_{r_1, r_2}^{p, p} = 1$. The clustering of cosmic large scale structure in the nonlinear regime essentially is due to the interaction between the modes of fluctuations on different scales (e.g., Peebles 1980). Therefore, it is important to detect the scale-scale correlation of cosmic baryon matter.

If the ratio r_2/r_1 is fixed, the log-Poisson hierarchy predicts the scale-scale correlation to be (Liu & Fang 2008)

$$C_{r_1, r_2}^{p, p} = B(r_2/r_1) r_1^{\xi(2p) - 2\xi(p)}, \quad (17)$$

where the factor $B(r_2/r_1)$ is constant when the ratio r_2/r_1 is fixed. This is because the log-Poisson model is invariant with respect to scale dilation. From eqs.(7) or (8), we have

$$\xi(2p) - 2\xi(p) = -\gamma(1 - \beta^p)^2 / (1 - \beta) \quad (18)$$

Thus, if r_2/r_1 remains constant, the relationship of $\ln C_{r_1, r_2}^{p, p}$ vs. $\ln r_1$ should be a straight line with slope $-\gamma(1 - \beta^p)^2 / (1 - \beta)$. This slope is also only dependent on the last term on the right hand side of eq.(8), regardless the parameter α .

3. Log-Poisson hierarchy of neutral hydrogen density field

Ly α absorption spectrum depends on the distribution of neutral hydrogen. We first study the mass density field of diffused neutral hydrogen. Since the UV background radiation is uniform and does not introduce special spatial scale, one may expect that the mass density field of neutral hydrogen is also a field of the log-Poisson hierarchy. However, the ratio of the neutral hydrogen density $\rho_{\text{HI}}(\mathbf{x})$ to total hydrogen density $\rho_{\text{H}}(\mathbf{x})$ is not spatially constant, because the temperature-density relation is of multiphase (He et al 2004, 2005). Therefore, the mass field of the neutral hydrogen would not have the same log-Poisson hierarchical features as of $\rho(\mathbf{x})$.

3.1. Simulation samples

The simulation samples of the fields of baryon fluid are generated by the same way as Liu & Fang (2008), which is based on the hybrid hydrodynamic N-body code of Weighted Essentially Non-oscillatory (WENO) scheme (Feng et al. 2004). It is in Eulerian scheme and suitable to analyze the fluid in high as well as in low mass density areas. The WENO samples have been successfully applied to reveal the self-similar hierarchy behavior of cosmic baryon fluid (Kim et al. 2005; He et al. 2006; Liu & Fang 2008), to explain the HI and HeII Ly α absorption in quasar spectra (Liu et al. 2006), and to study the relation between X-ray luminosity and temperature of groups of galaxies (Zhang et al. 2006). It is also used for studying Ly α leaks at high redshift (Liu et al. 2007).

The simulation is performed in a comoving cubic box of $100 h^{-1}$ Mpc with 512^3 grids and an equal number of dark matter particles. The grid size is $100/512 \sim 0.2 h^{-1}$ Mpc, which is less than Jeans length, and therefore, it is enough to catch the statistical behavior in the scale-free range, i.e. larger than the Jeans length and less than non-linear scale. We use the concordance Λ CDM cosmology model with parameters $\Omega_{\text{m}}=0.27$, $\Omega_{\text{b}}=0.044$, $\Omega_{\Lambda}=0.73$, $h=0.71$, $\sigma_8=0.84$, and spectral index $n = 1$. The transfer function is calculated using CMBFAST (Seljak & Zaldarriaga 1996). We take a primordial composition of H and He ($X=0.76$, $Y=0.24$).

The ionization fraction is calculated with ionization-recombination equilibrium under a uniform UV radiative background, of which the intensity is adjusted to fit the mean of observed Ly α transmitted flux. We produce the distributions of the mass density of hydrogen $\rho(\mathbf{x})$, the fraction of neutral hydrogen $f_{\text{HI}}(\mathbf{x})$, temperature $T(\mathbf{x})$, and velocity $\mathbf{v}(\mathbf{x})$ at redshift $z \simeq 2.5$, which is the mean redshift of observed samples used in §4.

We randomly sample 10,000 one-dimensional sub-samples to simulate the Ly α trans-

mitted flux (§4). To estimate the errors, we divided the 10,000 samples into 10 subsamples, each of which has 1,000 line samples.

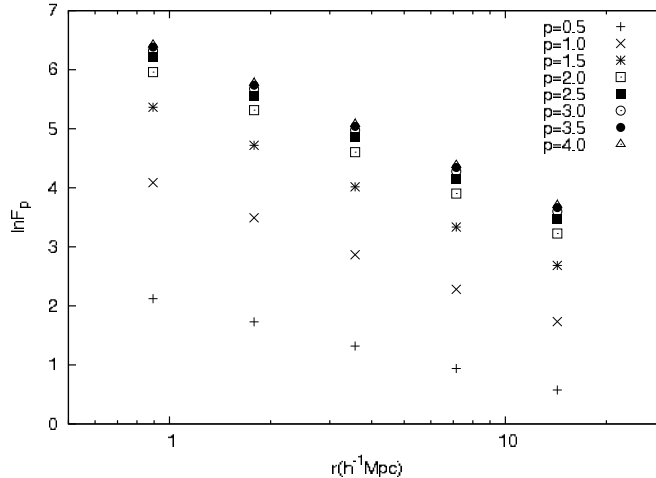


Fig. 1.— Function $F_p(r)$ vs. r of simulation samples of the mass density field of neutral hydrogen in the scale range $0.9 < r < 15 \text{ h}^{-1} \text{ Mpc}$, and $p = 0.5 \times n$, with $n = 1, 2 \dots 8$ from bottom to top.

3.2. Log-Poisson hierarchical statistics

The variable $\delta\rho_r = \rho(\mathbf{x} + \mathbf{r}) - \rho(\mathbf{x})$ of density field $\rho(\mathbf{x} + \mathbf{r})$ can be calculated by a discrete wavelet transform (DWT) as

$$\delta\rho_{r,l} = \int \rho_{\text{HI}}(x)\psi_{j,l}(x)dx, \quad (19)$$

where $\psi_{j,l}(x)$ is the base of discrete wavelet transform (e.g. Fang & Thews 1998). For a one-dimensional sample in physical space from $x = 0$ to L , the scale index j is related to the scale r by $r = L/2^j$ and the position index l is for the cell located at $x = lL/2^j$ to $(l + 1)L/2^j$. Because the DWT bases $\psi_{j,l}(x)$ are orthogonal, the variables $\delta\rho_{r,l}$ do not cause false correlation. They are effective to describe turbulence of fluid (Farge 1992). For a given scale r or j , the statistical average $\langle \dots \rangle$ of eq.(5) is over all cells l . We will use the Harr wavelet to do the calculation below. We also repeat the calculations with wavelet Daubechies 4.

Figures 1 - 3 demonstrate that the density field $\rho_{\text{HI}}(\mathbf{x})$ of neutral hydrogen shows the features of log-Poisson hierarchy. Figure 1 shows the functions $F_p(r)$ of the field ρ_{HI} in the physical length scale range $0.9 < r < 15 \text{ h}^{-1} \text{ Mpc}$ and orders of $p = 0.5 \times n$ with $n = 1, 2 \dots 8$. For all p , $\ln F_p(r)$ can be well fitted by a straight line of $\ln r$. It is consistent

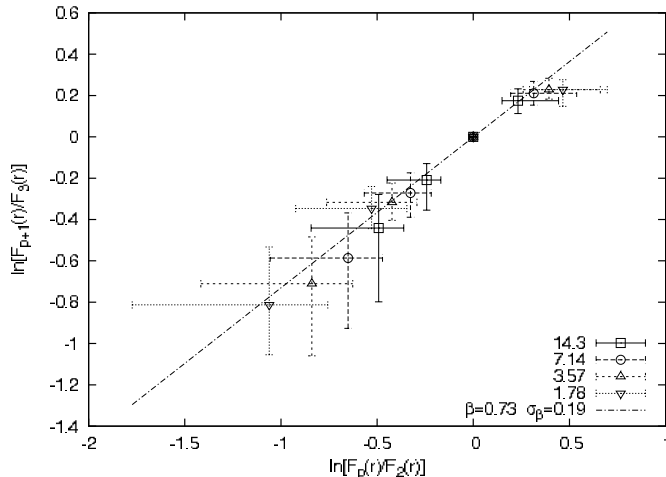


Fig. 2.— $\ln[F_{p+1}(r)/F_3(r)]$ vs. $\ln[F_p(r)/F_2(r)]$ for simulation samples of the mass density field of neutral hydrogen. The data points are on scales $r = 1.78, 3.57, 7.14$ and $14.3 \text{ h}^{-1} \text{ Mpc}$ and the statistical order to be $p = 1, 1.5, 2,$ and 2.5 .

with eq.(10). When $p > 3$, $F_p(r)$ given in Figure 1 is almost independent of p . This indicates that $F_p(r) \rightarrow F_\infty$ for higher p . Thus, from eq.(10), β should be less than 1, and therefore, the field is intermittent. In this case, the slope of the straight lines with higher p has to be equal to $-\alpha - \gamma$. Figure 1 shows $\alpha + \gamma = 1.0$.

Figure 2 is the β -hierarchy eq.(12) of the density field ρ_{HI} , in which the error bars are given by the ranges of $\ln[F_{p+1}(r)/F_3(r)]$ and $\ln[F_p(r)/F_2(r)]$ of the 10 subsamples, each of which consists of 1,000 lines. The β -hierarchy is held for all r in $1 < r < 15 \text{ h}^{-1} \text{ Mpc}$ and $p = 0.5$ to 4. It yields $\beta = 0.73 \pm 0.19$.

Figure 3 plots the intermittent exponent $\xi(p)$ [eq.(8)]. It shows that $\xi(p)$ can be well fitted with eq.(8) with parameters $\beta = 0.60$, $\alpha + \gamma = 1.0$ and $\alpha = 0.25$. These parameters are in agreement with that given by Figures 1 and 2. The error bars of Figure 3 are also the range of the 10 subsamples. Therefore, the HI mass density distribution in the scale range of ~ 1 to $15 \text{ h}^{-1} \text{ Mpc}$ can also be described by the log-Poisson hierarchy. However, the parameters β and γ are different from that of density field $\rho(\mathbf{x})$, which has $\beta \simeq 0.47$, and $\gamma \simeq 1$ (Liu & Fang 2008). That is, the density field $\rho_{\text{HI}}(\mathbf{x})$ is weaker intermittent and less singular than that of $\rho(\mathbf{x})$.

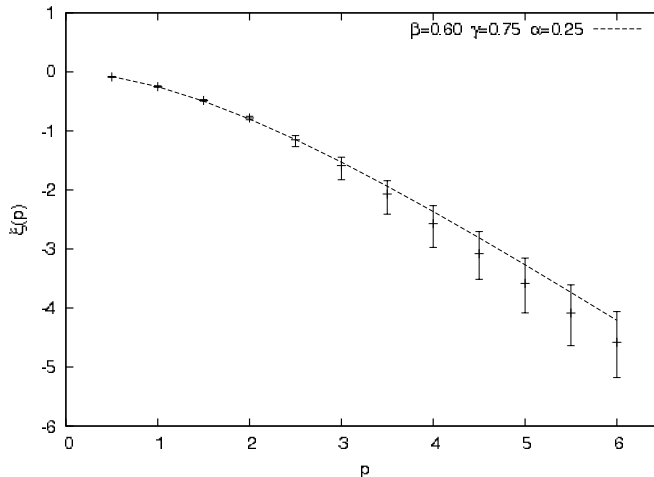


Fig. 3.— Intermittent exponent $\xi(p)$ of simulation samples of the mass density field of neutral hydrogen. The solid line is given by equation (8) with parameters $\alpha = 0.25$, $\beta = 0.60$ and $\gamma = 0.75$. The error bars are the variance of $\xi(p)$ over 10 samples, each of which contains of 1000 one-dimensional samples.

4. Log-Poisson hierarchy of Ly α transmitted flux

4.1. Samples

4.1.1. Observed data

For observed samples of Ly α transmitted flux, we use the high resolution, high signal to noise ratio QSO Ly α absorption spectra of Jamkhedkar (2002), Jamkhedkar et al. (2003). The power spectrum and intermittency of this data set have been extensively and deeply analyzed (Pando et al. 2002; Feng et al. 2002; Jamkhedkar et al.2003). It is useful for testing the log-Poisson hierarchy.

This observational data set consists of 28 Keck High Resolution (HIRES) QSO spectra (Kirkman & Tytler 1997). The QSO emission redshifts cover a redshift range from 2.19 to 4.11. The resolution is about 8 km s^{-1} . For each of the 28 QSOs, the data are given in form of pixels with wavelength, flux and noise. The noise accounts for the Poisson fluctuations in the photon count, the noise due to the background and the instrumentation. The continuum of each spectrum is given by IRAF CONTINUUM fitting.

The data are divided into 12 redshift ranges from $z = 1.6 + n \times 0.20$ to $1.6 + (n + 1) \times 0.20$ where $n = 0, \dots, 11$. In our analysis below, we use only the data in the range $z = 2.4$ to 2.6, which is the same as our simulation data. The scale range is taken to be 1.54 to 12.3

h^{-1} Mpc, which is also about the same as simulation samples. The mean flux in this redshift range is $\langle F \rangle \simeq 0.75$ (Jamkhedkar, 2002).

We use the same methods of Jamkhedkar et al. (2003) to deal with noises, metal lines, proximity effect, and bad data chunks. On average the S/N ratio of the Keck spectra is high. Most of the regions with low S/N are saturated absorption regions. Although the percentage of pixels within these regions is not large, they may introduce large uncertainties in the analysis. We should reduce the uncertainty given by low S/N pixels. The method is as follows. First, we calculate the SFCs (scaling function coefficients) of both transmission flux field $F(x)$ and noise field $n(x)$ with $\epsilon_{jl}^F = \int F(x)\phi_{j,l}(x)dx$ and $\epsilon_{jl}^N = \int n(x)\phi_{j,l}(x)dx$, where $\phi_{j,l}(x)$ is the scaling function of wavelet on scale j and at position l . We then identify unwanted mode (j, l) by using the threshold condition $|\epsilon_{jl}^F/\epsilon_{jl}^N| < f$. This condition flags all modes with S/N less than f . The parameter f is taken to be 3. We also flag modes dominated by metal lines. In order to easily flag data gaps, we set the flux at the gaps to be zero and the error to one, and do the same thing for pixels with negative flux. Finally, we skip all the flagged modes when doing statistics. With this method, no rejoining and smoothing of the data are needed.

4.1.2. Simulation samples

To simulate Ly α transmitted flux F , we use the 10,000 one-dimensional samples given in §3.1. For each 1-D sample, the transmitted flux of Ly α , $F(z)$ in redshift space is calculated with $F(z) = \exp[-\tau(z)]$, where $\tau(z)$ is the optical depth defined as

$$\tau(z) = \frac{\sigma_0 c}{H} \int_{-\infty}^{\infty} n_{\text{HI}}(x) V[z - x - v(x), b(x)] dx, \quad (20)$$

in which σ_0 is the effective cross-section of the resonant absorption; H is Hubble constant at the redshift of the sample, $n_{\text{HI}}(x)$ is the number density of neutral hydrogen atoms. The Voigt function is $V[z - x - v(x), b(x)] = 1/(\pi^{1/2}b) \exp\{-[z - x - v(x)]^2/b^2(x)\}$, and $b(x)$ being the thermal broadening. To have a proper comparison between simulation and observation, we add noises $n_i = G \times A_i$ to each pixel i , where G is randomly sampled from standard normal distribution and A_i is the noise level of pixel i . We then take the same data reduction of noised modes as observed data.

4.2. Redshift distortion and β -hierarchy

The velocity field $v(x)$ and thermal broadening $b(x)$ of eq.(20) will lead to the deviation of the statistical properties of $\ln F(z) = -\tau(z)$ from $n_{\text{HI}}(x)$ or $\rho_{\text{HI}}(x)$. The field $\ln F(z)$ is no longer to show all features of log-Poisson hierarchy. We should study which properties of the log-Poisson hierarchy can still be seen with Ly α transmitted flux.

Because the scale free range is larger than the Jeans length, the effect of thermal broadening would be small in this range. In this case, eq.(20) can be approximately as

$$-\ln F(z) = \tau(z) = \frac{\sigma_0 c}{H} \int n_{\text{HI}}(x) \delta[z - x - v(x)] dx. \quad (21)$$

This relation actually is a mapping from a physical space field $n_{\text{HI}}(x)$ to redshift space field $\tau(z)$, which is the same as that used in the redshift distortion of galaxy distribution. It has been shown that, with the DWT variables, the redshift distortion of eq.(21) can be estimated by (Yang et al 2002)

$$\delta\tau_{r,l} = \mathfrak{R}_r \delta\rho_{r,l}, \quad (22)$$

where the DWT variables $\delta\tau_{r,l}$ are given by $\delta\tau_{r,l} = \int \tau(x) \psi_{j,l}(x) dx = \int [-\ln F(x)] \psi_{j,l}(x) dx$. The redshift distortion factor \mathfrak{R}_r depends on the DWT power spectrum of the velocity field $v(x)$ on scale $r = L/2^j$.

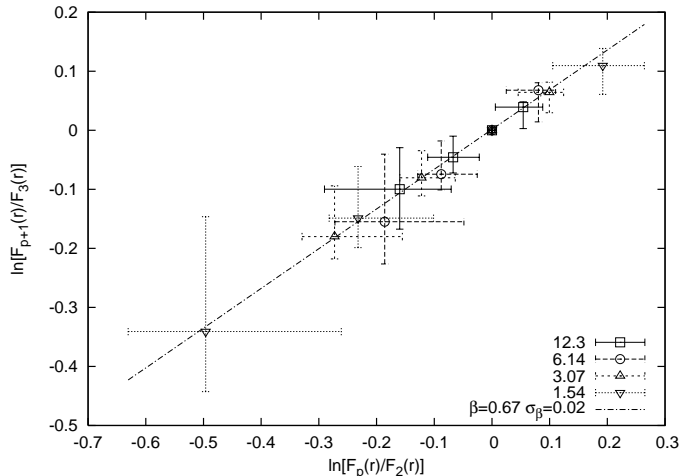


Fig. 4.— The β -hierarchy of observed sample of the Ly α transmitted flux at redshift $z = 2.4 - 2.6$ and physical scale range from ~ 1 to $15 \text{ h}^{-1} \text{ Mpc}$. The error bars are given by the maximum and minimum of bootstrap resampling.

Because the average of $\langle \dots \rangle$ in the structure function eq.(1), or $S_p(r = L/2^j) = \langle |\delta\rho_{j,l}|^p \rangle$, is only over on modes l , the redshift distortion factor \mathfrak{R}_r does not involve in this average.

Thus, the function $F_p(r)$ of $\delta\tau_{r,l}$ will be different from the function $F_p(r)$ of $\delta\rho_{r,l}$ by a factor \mathfrak{R}_r . Thus, both $F_{p+1}(r)/F_3(r)$ and $F_p(r)/F_2(r)$ of $\delta\tau_{r,l}$ do not contain the redshift distortion factor \mathfrak{R}_r . Thus, $F_{p+1}(r)/F_3(r)$ and $F_p(r)/F_2(r)$ of $\delta\tau_{r,l}$ should also satisfy the β -hierarchy eq.(12) as that of field ρ_{HI} . That is, the β -hierarchy is not affected by the redshift distortion.

Figure 4 presents the β -hierarchy of observed transmitted flux $F(z)$. It is very well fitted by a straight line for data on the scale range from ~ 1 to $15 \text{ h}^{-1} \text{ Mpc}$. It yields $\beta = 0.67 \pm 0.02$. Figure 5 shows the β -hierarchy of observed transmitted flux, which is the same as Fig.4, and the noised simulation samples F . We see that the both real and simulation samples are well coincident. The simulation samples yield $\beta = 0.66 \pm 0.02$. Therefore, both real and simulation samples are well β -hierarchical, and the numbers of β are well consistent.

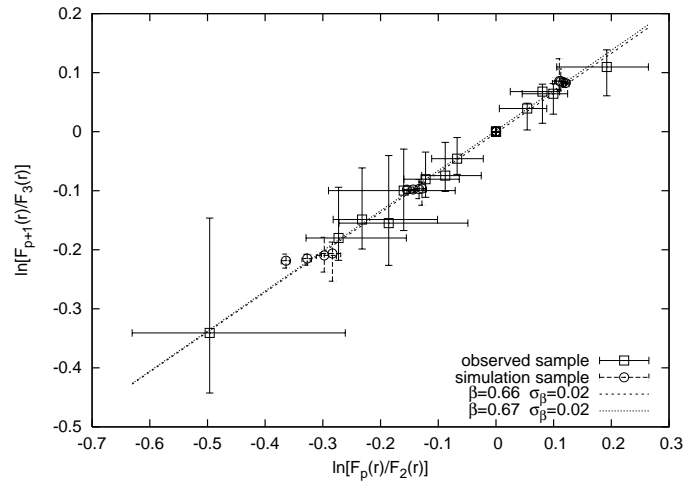


Fig. 5.— The β -hierarchy for a. observed data (square) as Fig. 4; b. simulation sample (circle) of the Ly α transmitted flux at redshift $z = 2.5$ and Gaussian noises are added with the same level as real data.

The data points of Figure 4 are scattered along the straight line $F_{p+1}(r)/F_3(r) - F_p(r)/F_2(r)$, while the points of Figure 5 are clustered. This is due to all simulation samples have the same length, while for real samples consisting quasars with different redshift, we take only the sections of transmitted flux, which are in the redshift range $z \simeq 2.4 - 2.6$.

4.3. High order moments

The statistics of eq.(14) is based on the ratio between high order moment $\langle \delta\rho_r^{2p} \rangle$ and $\langle \delta\rho_r^2 \rangle^p$, both of which have the same order of $\delta\rho_r$. When $p = 2$, the ratio actually is kurtosis. The moment ratio of $\langle \delta\tau_r^{2p} \rangle$ to $\langle \delta\tau_r^2 \rangle^p$, obviously, is independent of the redshift distortion

factor \mathfrak{R}_r . Therefore, the ratio of $\langle \delta\tau_r^{2p} \rangle$ to $\langle \delta\tau_r^2 \rangle^p$ has to satisfy the same property as $\langle \delta\rho_r^{2p} \rangle$ to $\langle \delta\rho_r^2 \rangle^p$. Thus, for a given p , the relation of $\ln\langle(\delta\tau_r)^{2p}\rangle/\langle(\delta\tau_r)^2\rangle^p$ and $\ln r$ has to be a straight line with slope $-\gamma[p(1 - \beta^2) - (1 - \beta^{2p})]/(1 - \beta)$ [eq.(15)]. Since the parameter β is already determined by the β -hierarchy, the test here is whether we can find one parameter γ to fit the slopes of $\langle \delta\tau_r^{2p} \rangle / \langle \delta\tau_r^2 \rangle^p$ vs. $\ln r$ for different p .

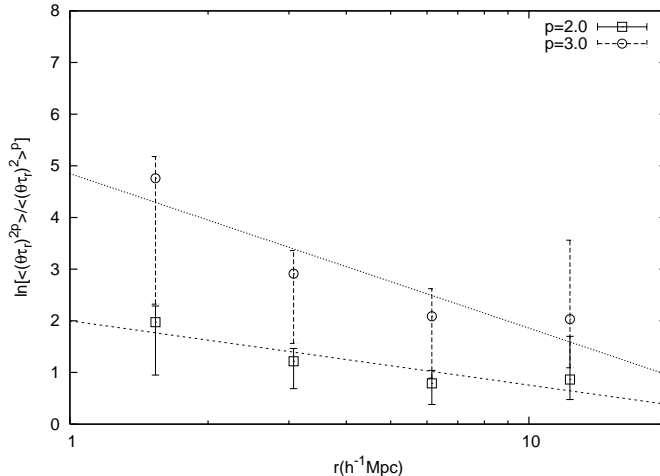


Fig. 6.— $\ln[\langle(\delta\tau_r)^{2p}\rangle/\langle(\delta\tau_r)^2\rangle^p]$ vs. r of real data in the scale range $\sim 1 - 15 h^{-1}$ Mpc, and p is taken to be 2 (bottom) and 3 (top). The solid lines are given by the least square fitting, which yield slopes 0.54 ± 0.19 ($p = 2$), and 1.3 ± 0.4 ($p = 3$). The error bars are given by the maximum and minimum of bootstrap resampling.

The result is presented in Fig. 6. It shows the relation of $\ln[\langle\delta\tau_r^{2p}\rangle/\langle(\delta\tau_r)^2\rangle^p]$ vs. $\ln r$ for real data with $p = 2$ and 3, i.e. the statistics are of the order of 4 and 6. The slopes of the fitted straight lines are 0.54 ± 0.19 for $p = 2$, and 1.3 ± 0.4 for $p = 3$. Thus, using $\beta = 0.67$, we have $\gamma = 0.59 \pm 0.20$ for $p = 2$ and $\gamma = 0.58 \pm 0.22$ for $p = 3$. In spite that the statistical errors are still large, one can already see that different p -lines yield about the same parameter γ . In other words, the moment statistics passed the test of log-Poisson hierarchy.

The number of γ given by the real data of the transmitted flux is less than the number $\gamma = 0.75$ of ρ_{HI} field (§3.2). Therefore, the field of transmitted flux of real samples is less singular than the field ρ_{HI} . This is reasonable if considering the real data are noised.

4.4. Log-Poisson hierarchy and log-normal model

In §4.2 and 4.3., we have found that the log-Poisson parameters of the transmitted flux should be $\beta = 0.67 \pm 0.02$ and $\gamma = 0.58 \pm 0.22$. This result can be used to com-

pare the log-Poisson hierarchy and log-normal model. We now consider the moment ratio $\ln[\langle\delta\tau_r^{2p}\rangle/\langle(\delta\tau_r)^2\rangle^p]$ as a function of p on a given scale r .

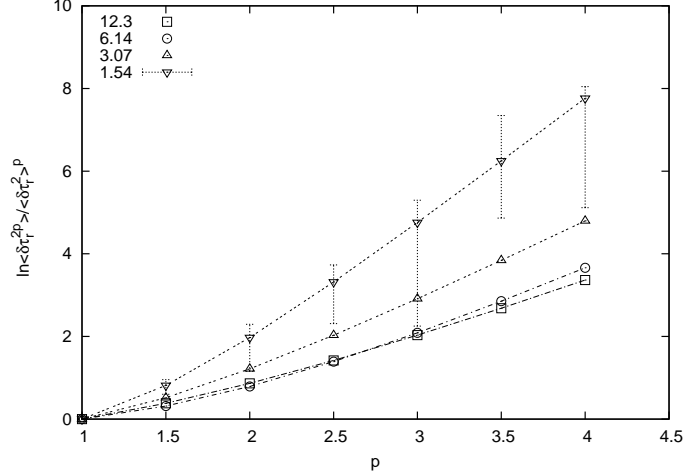


Fig. 7.— $\ln\langle\delta\tau_r^{2p}\rangle/\langle\delta\tau_r^2\rangle^p$ as a function of p for real data of Ly α transmitted flux at the range $z \sim 2.4 - 2.6$ on physical scales $r = 1.54$ (nabla), 3.07 (triangle), 6.14 (circle) and 12.3 (square) h^{-1} Mpc. The curves are from the fitting of log-Poisson model. For clarity, we show only the error bars for data points of $r = 1.54 h^{-1}$ Mpc. The errors of other r are about the same level as $r = 1.54 h^{-1}$ Mpc.

Figure 7 presents the $\langle\delta\tau_r^{2p}\rangle/\langle\delta\tau_r^2\rangle^p$ as a function of p for real data on scales $r = 1.54$ (nabla), 3.07 (triangle), 6.14 (circle) and 12.3 (square) h^{-1} Mpc. p is from 1 to 4. The p -dependent curves shown in Figure 7 are given by eqs.(14) and (15), in which the fitted parameters are $\beta = 0.67 \pm 0.02$ and $\gamma = 0.55 \pm 0.10$. The *const* in eq.(14) is determined by $\ln[\langle\delta\tau_r^{2p}\rangle/\langle\delta\tau_r^2\rangle^p] = 0$ when $p = 1$.

Although the observed data points of Figure 7 actually are the same as Figure 6, we see that the observed data points show large scatter in Figure 6, but almost no scatter in Figure 7. This is because Figure 6 gives moment ratio as a r function, while Figure 7 shows the p -dependence of the moment ratio. For a given r , the Gaussian noise will yield a moment ratio given by eq.(13), which is a smooth function of p . Therefore, a Gaussian noisy sample should not cause scatter with respect to p . On the other hand, Gaussian noise generally is not a smooth function of r . It yields the scatter of Fig. 6.

Figure 7 shows that the p -dependence of moment ratio $\ln[\langle\delta\tau_r^{2p}\rangle/\langle\delta\tau_r^2\rangle^p]$ is significantly dependent on scale r . Therefore, it can not be fitted by a Gaussian field, for which moment ratio is r -independent [eq.(13)]. The field of $\delta\tau$ is non-Gaussian. The smaller the scale r , the stronger the non-Gaussianity.

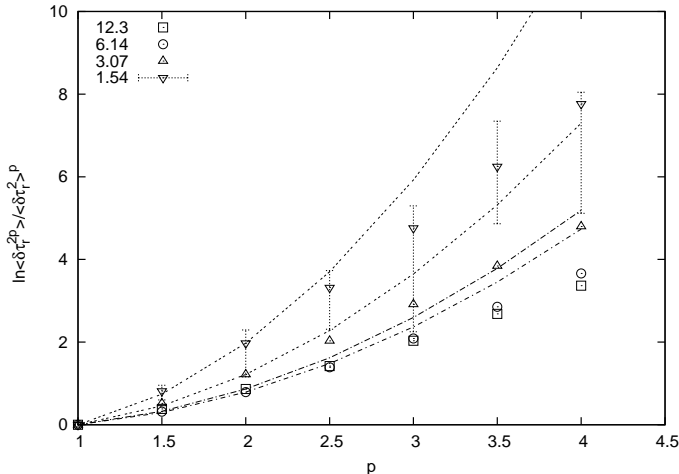


Fig. 8.— The same as Figure 7, but the curves are from the fitting of log-normal model.

The log-normal model of the transmitted flux of QSO Ly α absorption spectrum is very successful to explain various low-order statistical features of Ly α forests (Bi 1993; Bi & Davidsen 1997). The log-normal model also predicts that the transmitted flux is non-Gaussian and intermittent. For the moment ratio, the log-normal model yields (Pando et al 2002)

$$\frac{\langle \delta\tau_r^{2p} \rangle}{\langle \delta\tau_r^2 \rangle^p} = \exp[2(p^2 - p)\sigma^2(r)] \quad (23)$$

where $\sigma^2(r)$ is the power spectrum of the field. For each r , one can fit eq.(24) to observed points with $\sigma^2(r)$. The results are plotted in Figure 8. It shows that, if we try to give a good fitting of eq.(24) with real data at orders $p \leq 2$, the p -curves of eq.(24) always give a large deviation from the real data at $p > 2$. This deviation cannot be reduced with selecting $\sigma^2(r)$. This is because the deviation is from the p^2 -dependence of $\langle \delta\tau_r^{2p} \rangle / \langle \delta\tau_r^2 \rangle^p$ when p is large. The p^2 -dependence cannot be reduced with the parameter $\sigma^2(r)$.

On the other hand, at high p , the log-Poisson model gives $\langle \delta\tau_r^{2p} \rangle / \langle \delta\tau_r^2 \rangle^p \propto p$. The increasing with p is then consistent with observation. In Figs. 7 and 8 we show the error bars for data points of $r = 1.54 \text{ h}^{-1} \text{ Mpc}$. Although the errors are large at high p , the result is clearly consistent with p -dependence, and unfavourable to the p^2 -dependence. Therefore, the higher order statistics of the Ly α transmitted flux is effective to discriminate between the log-Poisson and the log-normal model. The log-normal model yields too strong non-Gaussianity. This point actually has already been mentioned in the study of turbulence (e.g. Frisch 1995).

4.5. Scale-scale correlation

The last statistical feature used to test the log-Poisson hierarchy is the scale-scale correction. Similar to the statistics of high order moment (§4.3), the ratio of scale-scale correction, $\langle \delta\tau_{r_1}^p \delta\tau_{r_2}^p \rangle / \langle \delta\tau_{r_1}^p \rangle \langle \delta\tau_{r_2}^p \rangle$ is independent of the redshift distortion factor \mathfrak{R}_r . The field τ should show the scale-scale correlation as ρ_{HI} eqs.(17)-(19).

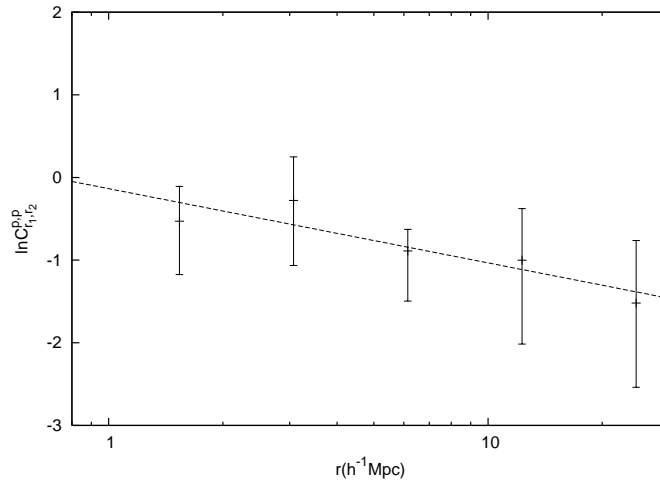


Fig. 9.— Scale-scale correlation of observed data of Ly α transmitted flux at the range $z \sim 2.4 - 2.6$ for $p = 2$ and $r_2/r_1 = 2$. The error bars are given by the maximum and minimum of bootstrap resampling.

Before doing this test, we would emphasize that the scale-scale correlation is statistically independent of the statistics of high order moments. For instance, one can construct a field, which shows Gaussian distribution in terms of its one point distribution of $\delta\rho_{j,l}$, but highly scale-scale correlated between variables $\delta\rho_{j,l}$ with different j (Pando et al 1998, Feng & Fang 2000). The clustering of cosmic large scale structure in the nonlinear regime essentially is due to the interaction between Fourier modes on different scales. Therefore, cosmic clustering will definitely leads to scale-scale correlation. Scale-scale correlation is also very effective to distinguish various hierarchy cascade models (Pando et al. 1998).

Figure 9 presents the $p = 2$ scale-scale correlation of observed data, in which the ratio r_2/r_1 is fixed to be equal to 2. The slop of the fitting straight line in Fig. 9 should be given by eq.(19). Since eq.(19) depends only on the parameters β and γ , both of which have already been determined in §4.2 and 4.3. There is no free parameters in the fitting of Fig. 9. If we doing a straight line, we found the parameters $\beta = 0.67$ and $\gamma = 0.43 \pm 0.12$. The value of β is the same as that of §4.2, while the value of γ is smaller than that of §4.3, but the deviation is not larger than $1-\sigma$. The scale-scale correlation is more sensitive to the quality

of the data, as it is the correlation between modes on different scales. The result of Figure 9 is basically consistent with the scale-scale correlation predicted by the log-Poisson hierarchy.

5. Discussion and conclusion

Nonlinear evolution of mass and velocity fields is a central problem of large scale structure of the universe. The clustering of the cosmic baryon fluid, governed by the Navier-Stokes equation in gravitational field of an expanding universe, has to be self similarly hierarchical in the scale free range in which the dynamical equations and initial perturbations are scale-invariant.

The log-Poisson hierarchical clustering sketches the nonlinear evolution of cosmic baryon fluid in the scale free range. If the initial density perturbations are Gaussian, and their power spectrum is given by power law $P(k) \propto k^\alpha$, the structure functions initially have to be $S_p(r) \propto r^{-p\alpha/2}$. In the regime of linear evolution, the structure functions will keep to be $S_p(r) \propto r^{\xi_l(p)}$, and the intermittent exponent is $\xi_l(p) = -p\alpha/2$. According to the log-Poisson hierarchy scenario, the nonlinear evolution leads to the hierarchical transfer of the power of clustering from large scales to small scales. The structure function will become $S_p(r) \propto r^{\xi_l(p)+\xi_{nl}(p)}$, where the nonlinear term of the intermittent exponent is $\xi_{nl}(p) = -\gamma[p - (1 - \beta^p)/(1 - \beta)]$, in which the parameters β and γ are dimensionless. β measures the intermittency of the field, and γ measures the singularity of the clustering. For Gaussian field, we have $\beta = 1$, and therefore, $\xi_{nl}(p) = 0$ for all order p . Since the onset of nonlinear evolution, the parameter β will gradually decrease, and the field becomes intermittent.

With simulation samples, we found that the parameter β is decreasing with the decrease of redshift z . It means that the field is weakly intermittent at earlier time, but strong intermittent at later time (Liu & Fang 2008). Although $\xi_{nl}(p) \neq 0$, the nonlinear evolution keeps the cosmic baryon fluid to be scale-invariant. We showed that the mass density field of neutral hydrogen fluid in the scale free range is also well described by the log-Poisson hierarchy in spite of the neutral hydrogen fraction of the baryon fluid is not constant in space. This is because the UV ionization photon is assumed to be uniform, and it does not violate the scale invariance of this system. However, the number of β of neutral hydrogen is found to be less than that of total baryon fluid. Therefore, the neutral hydrogen is less intermitted.

The Ly α transmitted flux of quasars Ly α absorption spectrum is considered to be effective to probe the mass and velocity fields of neutral hydrogen. However, the redshift distortion of the velocity field leads to the deviation of the field of the Ly α transmitted flux

from the neutral hydrogen field. The transmitted flux does not satisfy all predictions of log-Poisson hierarchy. Fortunately, the effect of redshift distortion is approximately negligible for some log-Poisson hierarchical predicted features. Thus, we can test the log-Poisson hierarchy with quasars Ly α absorption spectrum.

Using high resolution and high S/N data of quasars Ly α absorption spectrum, we show that all the non-Gaussian features predicted by the log-Poisson hierarchy, including the hierarchical relation, the intermittent exponent, the ratios of different moments, and the scale-scale correlation, are consistent with observed samples. The observed samples of the transmitted flux yield the same intermittence parameter β as that of neutral hydrogen field produced with hydrodynamic simulation of the concordance Λ CDM universe. Our result shows that the intermittent exponent $\xi(p)$, or parameters β and γ , is effective to discriminate among models of nonlinear evolution.

The log-normal model can well fit observed data on lower order statistics, but not good on higher orders. On the other hand, the log-Poisson model gives good fitting on lower order as well as higher order statistics. Therefore, a comparison between the log-Poisson model and log-normal model on lower order statistics will be able to find the relation between parameters of the log-Poisson and log-normal models. This relations would be useful to explain the parameters of log-Poisson model with well-known parameters in cosmology, as the parameters of log-normal model generally are known in cosmology.

Recent studies have shown that the turbulence behavior of baryon gas can be detected by the Doppler-broadened spectral lines (Sunyaev et al. 2003; Lazarian & Pogosyan 2006). Although these works focus on the turbulence of baryon gas in clusters, the result is still applicable, at least, for the warm-hot intergalactic medium (WHIM), which is shown to follow the evolution of Burger's fluid on large scales (He et al. 2004, 2005). The last but not least, the polarization of CMB is dependent on the density of electrons, and therefore, the map of CMB polarization would provide a direct test on the non-Gaussian features of ionized gas when the data on small scales become available.

We thank Ji-Ren Liu for his contributions in the early stage of this project. Y. Lu is supported by China Scholarship Council. This work was partially supported by US NSF AST 05-07340.

REFERENCES

Bec, J. & Frisch, U. 2000, Phys. Rev. E61, 1395

- Berera, A. & Fang, L.Z., 1994, *Phys. Rev. Lett.*, 72, 458
- Bi, H. G., 1993, *ApJ*, 405, 479
- Bi, H.G. & Davidsen, A.F. 1997, *ApJ*, 479, 523
- Bi, H.G., Ge, J. & Fang, L.Z., 1995, *ApJ*, 52, 90
- Boldyrev, S., Nordlund, A. & Padoan, P. 2002, *Phys. Rev. Lett.*, 89, 031102
- Cole, S. & Kaiser, N. 1988, *MNRAS*, 233, 637
- Davoudi, J., Masoudi, A.A., Tabar, M.R., Rastegar, A.R. & Shahbazi, F., 2001, *Phys. Rev. E* 63, 056308
- Dubrulle, B. 1994, *Phys. Rev. Lett.* 73, 959
- Fang, L.Z. & Feng, L.L. 2000, *ApJ*, 539, 5
- Fang, L.Z. & Thews, R. 1998, *Wavelets in Physics*, World Scientific (Singapore)
- Farge, M. 1992, *Ann. Rev. Fluid Mech.* 24, 395
- Feng, L.L. & Fang, L.Z. 2000, *ApJ*, 535, 519
- Feng, L.L. Shu, C.W. & Zhang, M.P., 2002, *ApJ*, 612, 1
- Feng, L.L., Pando, J., & Fang, L.Z., 2003, *ApJ*, 587, 487
- Feng, L.L., Shu, C.W., & Zhang, M.P. 2004, *ApJ*, 612, 1
- Frisch, U. 1995, *Turbulence*, Cambridge University Press
- Gurbatov, S. N., Saichev, A. I. & Shandarin, S. F., 1989, *MNRAS*, 236, 385
- He, P., Feng, L.L. & Fang, L.Z. 2004, *ApJ*, 612, 14
- He, P., Feng, L.L. & Fang, L.Z. 2005, *ApJ*, 623, 601
- He, P., Liu, J.R., Feng, L.L., Shu, C.W. & Fang, L.Z. 2006, *Phys. Rev. Lett.* 96, 051302
- Jamkhedkar, P. 2002, dissertation: Intermittency in the large scale structures of the universe, University of Arizona.
- Jamkhedkar, P., Zhan, H. & Fang, L.Z. 2000, *ApJ*, 543, L1

- Jamkhedkar, P., Feng, L.L., Zheng, W., Kirkman, D., Tytler, D., & Fang, L.Z., 2003, MNRAS, 343, 1110
- Jones, B.J.T. 1999, MNRAS, 307, 376
- Kim, B., He, P., Pando, J., Feng, L.L., & Fang, L.Z. 2005, ApJ, 625, 599
- Kirkman, D. & Tytler, D., 1997, ApJ, 484, 672
- Kolmogorov, A., 1941, Acad. Sci. USSR, 30, 301
- Laessig, M., 2000, Phys. Rev. Lett. 84, 2618
- Landau, L. D. & Lifshitz, E.M., 1987, Fluid Mechanics 2nd Ed., Pergamon Press.
- Lazrian, A. and Pogosyan, D. 2006, ApJ, 652, 1348
- Leveque, E. & She, Z.-S. 1997, Phys. Rev. E55, 2789
- Liu, J., Bi, H.G. & Fang, L.Z. 2007, ApJ, 671, L89
- Liu, J. & Fang, L. Z. 2008, ApJ, 672, 11
- Liu, J., Jamkhedkar, P., Zheng, W., Feng, L. L., & Fang, L. Z. 2006, ApJ, 645, 861
- Matarrese, S. & Mohayaee, R. 2002, MNRAS, 329, 37
- Monin, A.S. & Yaglom A.M., 1975, Statistical fluid mechanics: Mechanics of turbulence, Vol.2, (Cambridge, MIT Press)
- Padoan, P., Boldyrev, S., Langer, W. & Nordlund, A. 2003, ApJ, 583, 308
- Pando, J., Lipa, P., Greiner, M. & Fang, L.Z., 1998, ApJ, 496, 9
- Pando, J., Feng, L.L., Jamkhedkar, P., Zheng, W., Kirkman, D., Tytler, D., Fang, L.Z., 2002, ApJ, 574, 575
- Pando, J., Feng, L.L. and Fang, L.Z., 2004, ApJS, 154, 475
- Peebles, P. J. E. 1980, The Large-Scale Structure of the Universe, Princeton University Press
- Polyakov, A. M. 1995, Phys. Rev. E, 52, 6183
- Rauch, M. 1998, ARA&A, 36, 267
- Seljak, U. & Zaldarriaga, M. 1996, ApJ, 469, 437

- Shandarin, S.F. & Zeldovich, Ya. B. 1989, *Rev. Mod. Phys.* 61, 185
- She, Z. S. 1997, *Turbulence Modeling and Vortex Dynamics*, Lecture Notes in Physics, Volume 491. Springer-Verlag, p. 28
- She, Z.S. & Leveque, E., 1994, *Phys. Rev. Lett.* 72, 336
- She, Z.S. & Waymire, E.C., 1995, *Phys. Rev. Lett.* 74, 262
- Soneira, R. M. & Peebles, P. J. E. 1977, *ApJ*, 211, 1S
- Sunyaev, R.A., Norman, M.L. & Bryan, G.L. 2003, *Astronomy Letters*, 2, 783
- Yang, X. H., Feng, L. L., Chu, Y.Q. & Fang, L.Z.. 2002 *ApJ*, 566, 630
- Zhang, T.J., Liu, J.R., Feng, L.L., He, P. & Fang, L.Z., 2006, *ApJ*, 642, 625
- Zheng, W., et al., 2004, *ApJ*, 605, 631